14p

X-661-73-393
PREPRINT

NASA TM X-

MILLISECOND TEMPORAL STRUCTURE IN CYG X-1

R. E. ROTHSCHILD
E. A. BOLDT
S. S. HOLT
P. J. SERLEMITSOS

(NASA-TM-X-70583) MILLISECOND TEMPORAL STRUCTURE IN CYG X-1 (NASA) ~~13~~ 14 p HC $4.00 CSCL 03A

N74-17544

Unclas
G3/30 30793

DECEMBER 1973

GSFC

GODDARD SPACE FLIGHT CENTER
GREENBELT, MARYLAND

MILLISECOND TEMPORAL STRUCTURE IN CYG X-1

R. E. Rothschild+, E. A. Boldt, S. S. Holt and P. J. Serlemitsos
NASA/Goddard Space Flight Center
Greenbelt, Maryland 20771

ABSTRACT

Evidence is presented for the X-ray variability of Cyg X-1 on time scales down to a millisecond. Several "bursts" of millisecond duration are observed. The duty cycle for bursting is estimated to be $\geq 2 \times 10^{-4}$ averaged over the entire 49 second exposure, although the maximum burst activity is associated with a region of enhanced emission lasting about 1/3 second. Such bursts may be associated with turbulence in disk accretion at the innermost orbits for a black hole.

+NAS-NRC Resident Research Associate

MILLISECOND TEMPORAL STRUCTURE IN CYG X-1

I. INTRODUCTION

Millisecond and/or submillisecond pulses from an X-ray source have been advanced as possible observational evidence of a black hole (Shakura and Sunyaev, 1973, Leach and Ruffini, 1973, Pringle and Rees, 1972). Cyg X-1 is already known to display temporal structure on time scales down to several tens of milliseconds (Oda, et al., 1971, Rappaport, et al., 1971, Holt, et al., 1971, Schreier, et al., 1971). In this Letter we report the observation of millisecond bursts from Cyg X-1.

II. EXPERIMENT

On October 4, 1973 at 340 UT an X-ray astronomy payload was launched (flight number 13.010) from White Sands Missile Range in order to study the compact binary sources Her X-1, Cyg X-1 and Cyg X-3. The payload consisted of two multilayer multianode gas proportional counters with total effective viewing area of 1360 cm^2 and with 1-mil aluminized Kapton windows. Both detectors were filled to 1.1 atmospheres, one with 90% argon - 10% methane and the other with 90% xenon - 10% methane. The xenon detector had 3° circular collimation and an energy range of 1.5 - 35 keV while the argon detector had 2° x 8° collimation and an energy range of 1.5 - 20 keV.

Events were accepted as bona fide X-ray interactions if no coincidence between layers were present and if the collected charge were less than the upper threshold set to veto heavily ionizing events. The basic telemetry format consisted of contiguous 20.48 ms frames, each containing 64 words of 320 μs duration. The first event accepted during each word time was pulse-height analyzed and digitized into one of 128 PHA channels. This event and

subsequent ones accepted during a word time were also accumulated by a 5-bit scaler with dead time of $\leqslant 3\ \mu$sec per event. Rejected event counts were scaled every 20.48 ms and read out every frame.

The attitude of the rocket was controlled by a STRAP IV (Shrewsberry, et al., 1973) pointing system, which, during the exposure to Cyg X-1, aimed the detectors to within 15 arcminutes of the programmed direction. This eliminated any appreciable modulation of the count rate due to motion of the rocket while pointing.

III. DATA AND ANALYSIS

Figure 1 displays a comparison of data from each of the three sources observed. Even though they are all considered collapsed objects in binary systems, they posses quite different X-ray temporal profiles. Her X-1 exhibits clearly the 1.24 second pulsar period (Holt et al., 1974), while Cyg X-3 displays no such obvious temporal structure. The X-ray profile of Cyg X-1 shows considerable variability, qualitatively different from either of the other two sources.

During the exposure of Cyg X-1 the intensity experienced several periods of enhanced activity, especially from 318 to 319 seconds after launch (see Figure 2). During this time the counting rate increased from the overall mean value of 1274 counts/second to 2188 counts/second averaged over 409.6 ms (20 data frames) encompassing the enhancement of about 1/3 second duration. On three occasions during twenty milliseconds at the peak of the enhancement the instantaneous count rate for 1.28 ms samples increased to ≥ 12 counts/1.28 ms (≥ 9375 counts/second) (see Figure 3).

Poisson statistics, based on the mean rate of 2188 counts/second, would predict .01 such events during the 409.6 ms interval considered here.

Using the enhancement and bursts as a guide, the entire Cyg X-1 exposure was divided into 120 contiguous intervals of 409.6 ms duration, and each interval was divided into 320 1.28 ms bins. For each interval the mean count per bin was calculated and the counts for each bin noted. The expectation value N(n) for the number of bins containing n counts was determined for each interval using the mean count per bin for each interval and Poisson statistics. In each interval a count n^* was picked such that the expectation value for the number of bursts $N^* \equiv \sum_{n \geq n^*} N(n) \leq .01$, where n^* was the lowest integer possible. All bins in the interval were then examined to see how many had $n \geq n^*$. The result of this analysis, summed over all 120 intervals, was that in six intervals there existed at least one burst for which $n \geq n^*$. These six intervals contained eight bursts whereas the expectation value for the entire exposure is 0.73. The eight bursts in 49.2 seconds of exposure indicate a duty cycle of 2×10^{-4} for detectable bursts. The eight bursts described above yielded a total of 85 counts of which 22 were pulse height analyzed over the band 2 - 10 keV (where detection efficiency is high). The efficiency-corrected average photon energy in this interval was 4.1 keV, indicating that the bursts may have a harder spectrum (but not one substantially softer) than the overall source emission.

Adopting a technique similar to one brought to our attention by Oda (Oda, M., Matsuoka, M., Miyamoto, S., Ogawara, Y., and Takagishi, K., Memorandum 1973) an attempt was made to estimate the burst duration of

the eight bursts described above assuming they had a simple "on-off" pulse shape with fixed width. Data from 6.72 ms encompassing each burst were used to evaluate the non-burst background in each case. The ratio of the net counts in the peak bin to the net counts in the adjacent spillover bin, superposed over all eight bursts, is consistent with a burst width of .9 ms for trial bins of both .96 ms and 1.28 ms. The same analysis of just the three bursts shown in Figure 3 was consistent with the same result.

In evaluating the relative sensitivity of different rocket-borne experiments to millisecond bursts from Cyg X-1, it is important to note that if our detector area had been half as much as used in this experiment the analysis employed here for detecting bursts would have recognized none of the bursts actually observed.

In order to confirm the reliability of the above analysis, the data for Cyg X-3, (which had a mean count rate and exposure comparable to Cyg X-1) were examined for bursts and none were found. The rate of rejected (i.e., non X-ray) events was then examined during the time of the enhancement, and no significant variations were seen. This then minimizes the chance that the bursts were due to pick-up in the electronics from such things as attitude control valves firing or camera relays changing state. Finally, the combined rate from the inner layers of the argon detector was compared with the first layer rates from both detectors, and all three sets of data were similar within the statistical accuracy available. This eliminates the possibility that precipitating energetic electrons entering through the windows were responsible for the observed bursts.

IV. DISCUSSION

When there is disk accretion surrounding a black hole, fluctuations of the observed luminosity arising from turbulence may be expected (Shakura and Sunyaev, 1973) at a level given by

$$\frac{\Delta L}{L} \sim \frac{\dot{M}}{\dot{M}_{cr}} \alpha^2 \tag{1}$$

where $\dot{M}$ is the flux of matter, $\dot{M}_{cr}$ is the flux corresponding to the Eddington critical luminosity, and α is an efficiency parameter ($\alpha \leqslant 1$) for the mechanism of angular momentum transport. For $\alpha \sim 1$ and $\dot{M} \sim \dot{M}_{cr}$, we note that $\frac{\Delta L}{L}$ is on the order of unity. The typical time of these fluctuations is given by

$$\Delta t_f \sim \frac{10^{-4}}{\alpha} \frac{M}{M_\odot} \left(\frac{Rc^2}{6GM}\right)^{3/2} \text{ seconds} \tag{2}$$

where M is the mass of the black hole and R is the radial distance of the disturbance from the center of the black hole. For $R \geqslant R_o = \frac{6GM}{c^2}$ (the smallest stable orbit for the Schwarzchild metric), $M \geqslant 10M_\odot$, and $\alpha \leqslant 1$, we note that $\Delta t_f \geqslant 10^{-3}$seconds.

The loss of energy (U) corresponding to a mass (M) reaching the innermost stable orbit is given by

$$U = \eta Mc^2 \tag{3}$$

where η is the efficiency of gravitational energy release (e.g., $\eta \simeq .06$ for the case of the Schwarzschild metric and $\eta \simeq .42$ for the case of an extreme Kerr black hole). The corresponding release of energy in X-radiation would be given by

$$\Delta L \; \Delta t_f = \varepsilon U = \varepsilon \eta Mc^2 \tag{4}$$

where ε is the efficiency of the X-radiation process relative to all energy-loss mechanisms. For thermal emission ε approaches unity, whereas for non-

thermal emission $\varepsilon \approx 10^{-5}$.

The mass associated with the disturbances observed may be estimated by equation (4), viz:

$$10^5 > \frac{0.06Mc^2}{\Delta L_f \Delta t_f} \gtrsim 1 \qquad (5)$$

where ΔL_f is the luminosity increase during a fluctuation of duration Δt_f, and where we have taken $\eta = .06$. The lower limit corresponds to the situation where all energy transfer mechanisms channel their release into thermal X radiation (i.e., $\varepsilon \approx 1$). The upper limit corresponds to the non-thermal bremsstrahlung produced by particles transferring most of their energy to the ambient matter (i.e., $\varepsilon \approx 10^{-5}$). For disturbances where $\Delta t_f > 10^{-4}$ seconds (i.e. greater than the collision loss time), thermal radiation is likely to dominate, whereas for possible submillisecond structure, non-thermal radiation could be favored as the collision-loss time is approached.

Using equation (5) we obtain that for the largest millisecond burst (containing 13 counts in a 1.28 ms bin compared with an expectation value of 2.8 counts)

$$7 \times 10^{19}\,\mathrm{g} > M \gtrsim 7 \times 10^{14}\,\mathrm{g} \qquad (6)$$

whereas for the total associated time (~ 1/3 second) of enhanced activity, the corresponding composite mass involved becomes

$$2 \times 10^{21}\,\mathrm{g} > M \gtrsim 2 \times 10^{16}\,\mathrm{g}. \qquad (7)$$

These calculations assume the distance to Cyg X-1 to be 2.5 kpc (Margon, Bowyer and Stone, 1973). If we assume the infalling radial velocity is about 10^{-2} times the Keplerian orbital velocity (see Pringle and Rees, 1972), then the 1/3 second duration of the observed enhancement corresponds to the infall time for matter from 4 R_o to R_o (the radius of the innermost stable orbit) about a 10 $M_\odot$ black hole. The orbital velocities associated with this range of radii vary from $\beta = .2$ to $\beta = .4$. Particles undergoing velocity changes in this range are capable of producing the X-rays observed.

V. CONCLUSIONS

We have evidence of the variability of Cyg X-1 on time scales down to a millisecond, consistent with turbulence in disk accretion. The period of enhanced emission containing three of these bursts lasts for about 1/3 second, which is consistent with the infall time for matter from 4 R_o to R_o about a 10 $M_\odot$ black hole. The changes in luminosity associated with these three bursts are greater than six times the mean luminosity of the entire exposure. When the entire exposure to Cyg X-1 was examined, it was found that detectable bursts occurred ~ .02% of the time.

Recent mass determinations of Cyg X-1 (Brucato and Kristian, 1973, Hutchings, et al., 1973, Bregman, et al., 1973) place its minimum mass greater than the 3.2 $M_\odot$ upper limit for neutron stars of any type (Leach and Ruffini, 1973). If one assumes that variations in emission come from turbulence in accretion, then millisecond bursts imply (see equation (2)) that Cyg X-1 must have a radius less than 10^2 km (e.g., less than the radius of a white dwarf). This evidence combined with the mass determinations points toward a black hole nature for Cyg X-1.

ACKNOWLEDGEMENTS

It is a pleasure to acknowledge F. Birsa, C. Glasser, J. Saba and M. Ziegler for their technical support in carrying out this experiment. We also thank the sounding rocket group at Goddard Space Flight Center and the launch crew at White Sands Missile Range for their cooperation.

REFERENCES

Bregman, J., Butler, D., Kemper, E., Koski, A., Kraft, R. P., and Stone R. P. S., 1973, Ap. J. (Letters), 185, L117.

Brucato, R., and Kristian, J., 1973, Ap. J. (Letters), 179, L129.

Holt, S. S., Boldt, E. A., Schwartz, D. A., Serlemitsos, P. J., and Bleach R. D., 1971, Ap. J. (Letters), 166, L65.

Holt, S. S., Boldt, E. A., Rothschild, R. E., Serlemitsos, P. J., 1974, NASA-GSFC Document X-661-74-11

Hutchings, J., Crampton, D., Glaspey, J., and Walker, G., 1973, Ap. J. 182, 549.

Leach, R., and Ruffini, R., 1973, Ap. J. (Letters), 180, L15.

Margon, B., Bowyer, S., and Stone, R. P. S., 1973, Ap. J. (Letters), 185, L113.

Oda, M., Gorenstein, R., Gursky, H., Kellogg, E., Schreier, E., Tanabaum, H., and Giacconi, R., 1971, Ap. J. (Letters), 166, L1.

Pringle, J., and Rees, M., 1972, Astron. and Astrophys., 21, 1.

Rappaport, S., Doxsey, R., and Zaumen, W., 1971, Ap. J. (Letters), 168, L43.

Schreier, E., Gursky, H., Kellogg, E., Tananbaum, H., and Giacconi, R., 1971, Ap. J. (Letters), 170, L21.

Shakura, N., and Sunyaev, R., 1973, Astron. and Astrophys., 24, 337.

Shrewsberry, D., Budney, T., Riley, D., and Schuler, B., 1973, AAIA 3rd Sounding Rocket Technology Conference, AAIA No. 73-288.

FIGURE CAPTIONS

Fig. 1 Fifteen seconds of exposure to Her X-1, Cyg X-3, and Cyg X-1, respectively, binned every 20.48 ms. The inset shows the flight profile in counts/2 seconds versus seconds after launch. The horizontal arrows show where in the exposure to each source, the fifteen seconds of data occurred.

Fig. 2 The entire exposure to Cyg X-1 as a function of time. The count rates are binned every 20.48 ms. Cyg X-1 was acquired at 276 seconds after launch and the rocket doors started to close at 325 seconds after launch. The enhancement between 318 and 319 seconds after launch contains three of the observed bursts.

Fig. 3 Eighty milliseconds of exposure to Cyg X-1 containing the peak of the enhancement near 318 seconds after launch. The count rates are binned every 640 μs. Bursts with $\geq$ 12 counts/1.28 ms are shaded.

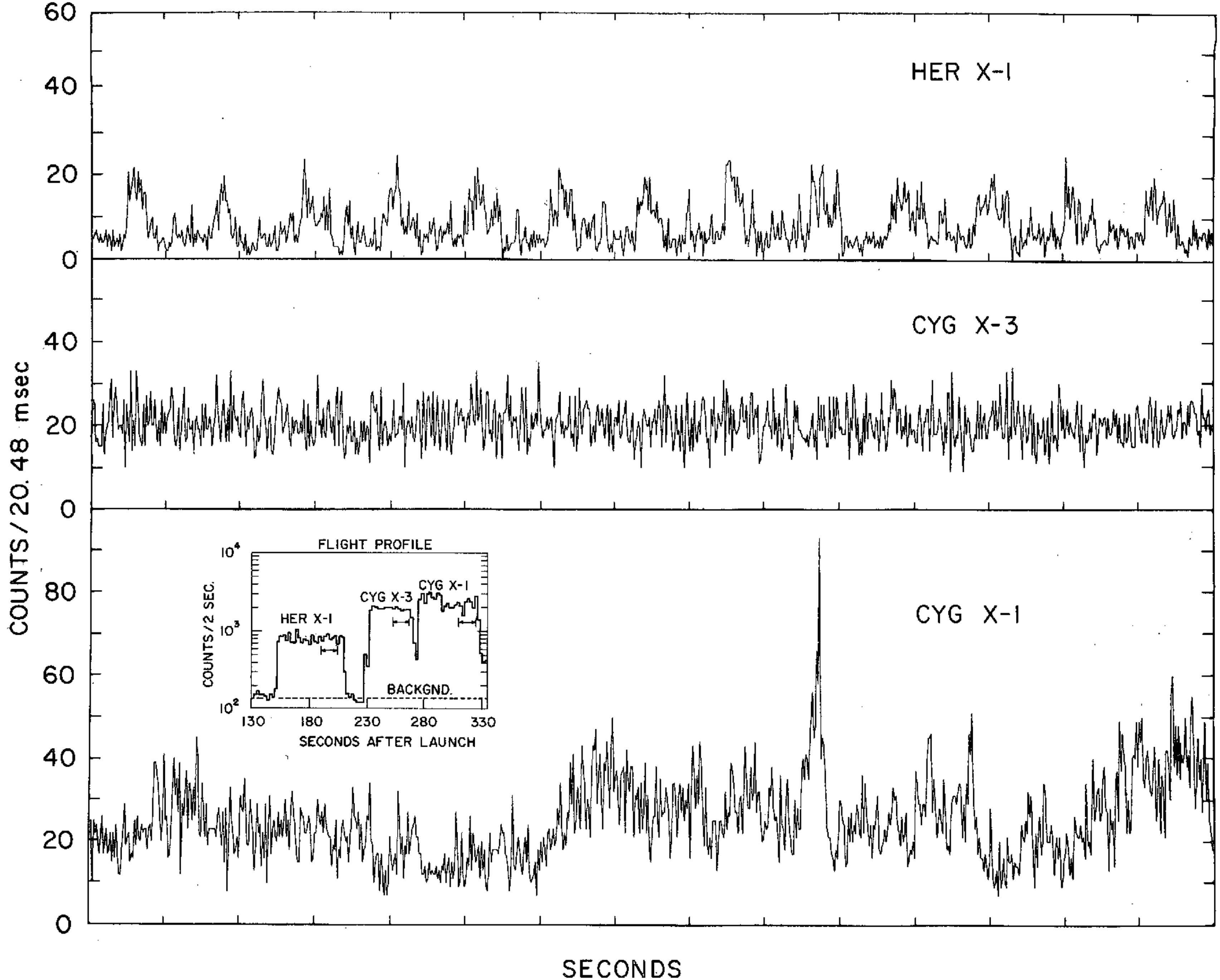
HER X-1
CYG X-3
CYG X-1
COUNTS/20.48 msec
SECONDS
FLIGHT PROFILE
COUNTS/2 SEC.
SECONDS AFTER LAUNCH
BACKGND.
130 180 230 280 330

16

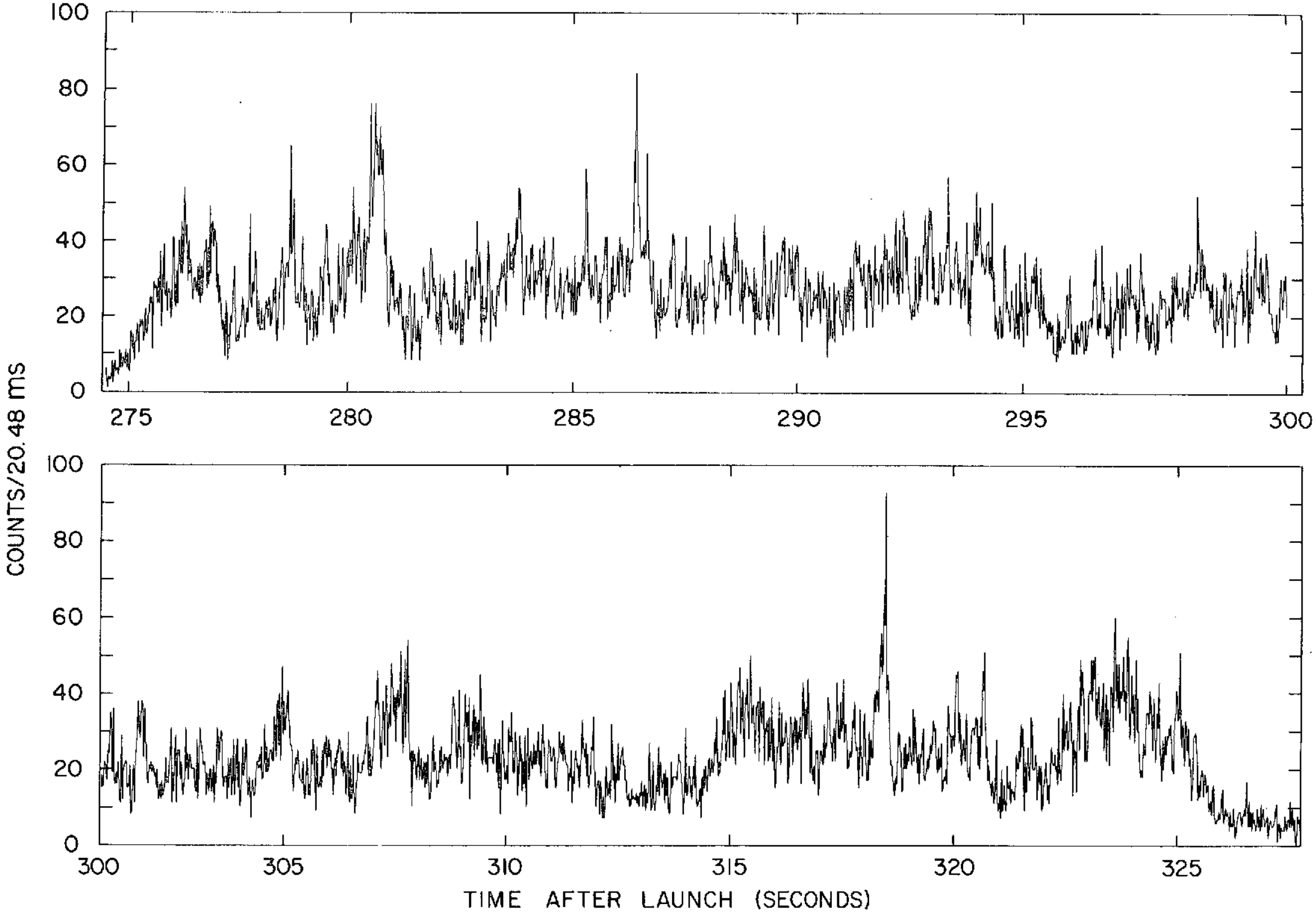

100
80
60
40
20
0
275
280
285
290
295
300
COUNTS/20.48 ms
305
310
315
320
325
TIME AFTER LAUNCH (SECONDS)

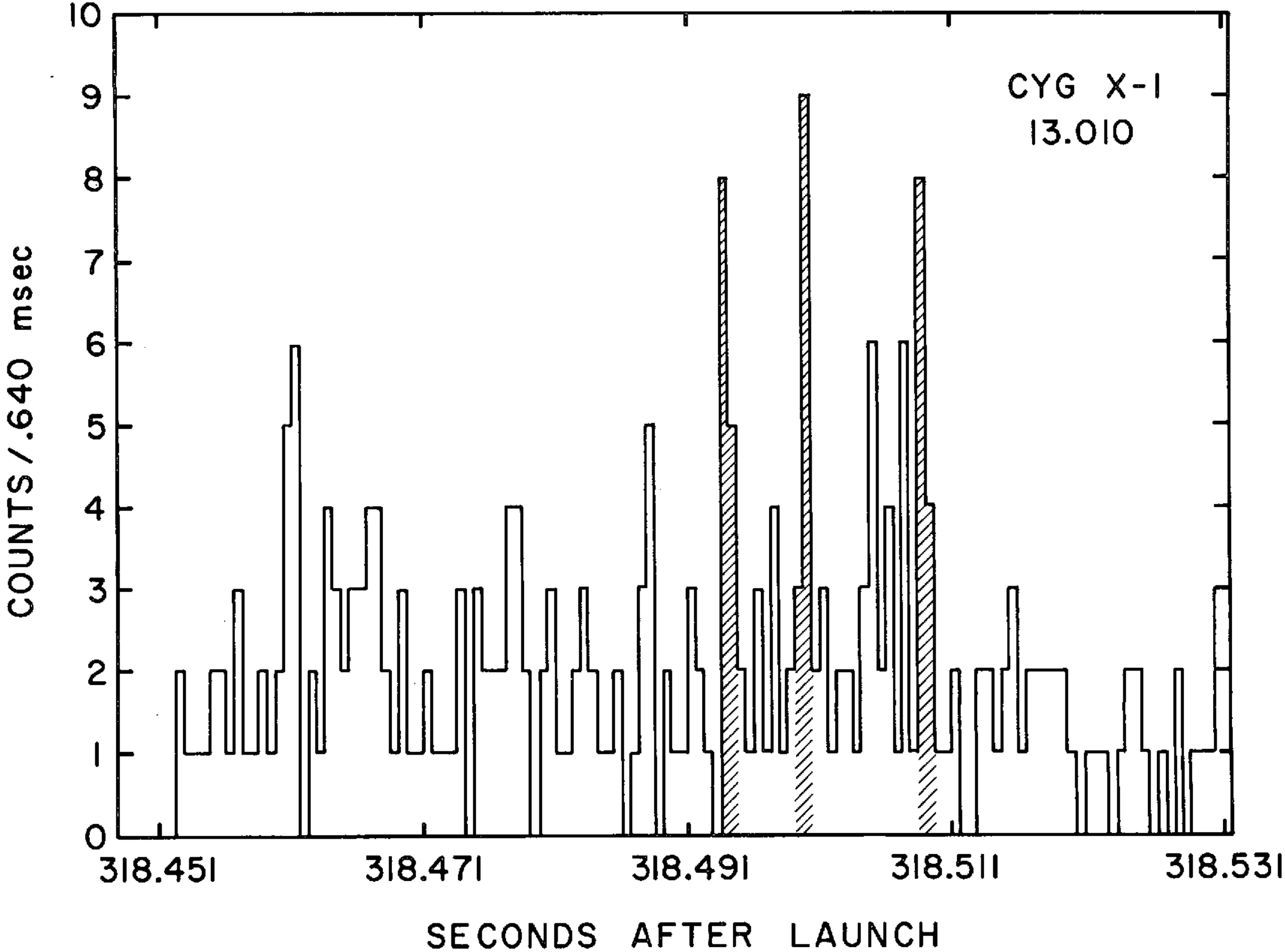
CYG X-1
13.010
COUNTS / .640 msec
0
1
2
3
4
5
6
7
8
9
10
318.451
318.471
318.491
318.511
318.531
SECONDS AFTER LAUNCH

NASA-GSFC